

Article

Research on Water Invasion Law and Control Measures for Ultradeep, Fractured, and Low-Porosity Sandstone Gas Reservoirs: A Case Study of Kelasu Gas Reservoirs in Tarim Basin

Dong Chen ¹, Chengze Zhang ¹, Min Yang ¹, Haiming Li ¹, Cuili Wang ¹, Pengxiang Diwu ², Hanqiao Jiang ^{3,4} and Yong Wang ^{3,4,*} 

¹ Tarim Oilfield Branch of PetroChina Company Limited, Korla 841000, China; 19390659699@163.com (D.C.); ybxwxybxf@126.com (C.Z.); yangmin_tlm@163.com (M.Y.); lhmztt8689@163.com (H.L.); wcl15982205106@163.com (C.W.)

² College of Science, China University of Petroleum, Beijing 102249, China; diwupx@cup.edu.cn

³ State Key Laboratory of Petroleum Resource and Prospecting, China University of Petroleum, Beijing 102249, China; jianghq@cup.edu.cn

⁴ College of Petroleum Engineering, China University of Petroleum, Beijing 102249, China

* Correspondence: wycupb@163.com

Abstract: The exploitation of ultradeep, fractured, and low-porosity gas reservoirs often encounters challenges from water invasion, exacerbated by the presence of faults and fractures. This is particularly evident in the Kelasu gas reservoir group, located in the Kuqa Depression of the Tarim Basin. The complexity of the water invasion patterns in these reservoirs demands a thorough investigation to devise effective water control measures. To elucidate the water invasion patterns, a combined approach of large-scale physical modeling and discrete fracture numerical simulations was adopted. These models allowed for the identification and categorization of water invasion behaviors in various gas reservoirs. Furthermore, production dynamic analysis was utilized to tailor water control strategies to specific invasion patterns. The large-scale physical simulation experiment revealed that water invasion in gas reservoirs is primarily influenced by high-permeability channels (faults + fractures), and that the gas production rate serves as the key factor governing gas reservoir development. The range of gas extraction rates spans from 3% to 5%. As the gas extraction rate increases, the extraction intensity diminishes and the stable production duration shortens. On the basis of the changes in the water breakthrough time and water production rate, a 2% gas extraction rate is determined as the optimal rate for the model. The embedded discrete fracture numerical simulation model further supports the findings of the physical simulation experiments and demonstrates that ① this type of gas reservoir exhibits typical nonuniform water invasion patterns, controlled by structural location, faults, and degree of crack development; ② the water invasion patterns of gas reservoirs can be categorized into three types, these being explosive water flooding and channeling along faults, uniform intrusion along fractures, and combined intrusion along faults and fractures; ③ drawing from the characteristics of water invasion in various gas reservoirs, combined with production well dynamics and structural location, a five-character water control strategy of “prevention, control, drainage, adjustment, and plugging” is formulated, with the implementation of differentiated, one-well, one-policy governance. The study concludes that a proactive approach, prioritizing prevention, is crucial for managing water-free gas reservoirs. For water-bearing reservoirs, a combination of three-dimensional water plugging and drainage strategies is recommended. These insights have significant implications for extending the productive lifespan of gas reservoirs, enhancing recovery rates, and contributing to the economic and efficient development of ultradeep, fractured, and low-porosity gas reservoirs.

Keywords: Kuqa Depression; fractured, low-porosity gas reservoirs; large physical simulation; embedded discrete fracture numerical simulation; gas production rate



Citation: Chen, D.; Zhang, C.; Yang, M.; Li, H.; Wang, C.; Diwu, P.; Jiang, H.; Wang, Y. Research on Water Invasion Law and Control Measures for Ultradeep, Fractured, and Low-Porosity Sandstone Gas Reservoirs: A Case Study of Kelasu Gas Reservoirs in Tarim Basin. *Processes* **2024**, *12*, 310. <https://doi.org/10.3390/pr12020310>

Academic Editors: Qingbang Meng and Qibin Li

Received: 10 January 2024

Revised: 23 January 2024

Accepted: 26 January 2024

Published: 1 February 2024



Copyright: © 2024 by the authors. Licensee MDPI, Basel, Switzerland. This article is an open access article distributed under the terms and conditions of the Creative Commons Attribution (CC BY) license (<https://creativecommons.org/licenses/by/4.0/>).

1. Introduction

In recent years, the demand for oil and gas energy has increased, the exploration and development of oil and gas in middle and shallow layers have become increasingly mature, and new explorations and discoveries in middle and shallow layers have become more and more difficult to make. Deep and ultradeep fields have gradually become the foci and hotspots of oil and gas exploration and development [1–5]. The ultradeep, fractured, and tight gas fields in the Kuqa Depression of Tarim Basin are the main bodies of natural gas production in Tarim Basin during the “14th Five-Year Plan period” in China. This type of gas field has large reserves, developed edge and bottom waters, deep burials, high temperatures, high pressures, and fractures that develop differently [6,7]. Since the major development of the ultradeep gas reservoirs in the Kuqa Depression in 2008, many large gas fields, such as Keshen 2, Dabei, Keshen 5, Keshen 8, and Keshen 9, have been discovered and established successively. At present, 29 gas reservoirs have been put into development and trial production. The total proven natural gas geological reserves submitted are more than $1 \times 10^{12} \text{ m}^3$, and the natural gas production capacity is $100 \times 10^8 \text{ m}^3$, and they have become the main gas sources of the “West–East Gas Transmission Project (Project of Natural Gas Transmission from West to East China)”. The main gas-bearing strata of the gas field group are the Cretaceous Bashijiqike Formation, with a buried depth of more than 6500 m, belonging to the category of ultradeep reservoirs [8–10]. Taking the Keshen gas reservoirs as examples, both are fractured, low-porosity sandstone gas reservoirs, and their production dynamics are very different. Under conditions of the same recovery degree, there are two cases of comprehensive flooding and good production. In essence, the geological characteristics and fracture modes of the two gas reservoirs are quite different [11,12].

In order to put forward effective control measures and means, on the basis of studying the geological characteristics of the gas reservoirs, combined with gas reservoir production performance, using embedded discrete fracture model numerical simulation (EDFM), among other means, a water invasion model of ultradeep, fractured, and tight gas reservoirs is established, considering the two factors of the fault and fracture development degrees [13,14]. It is applied to the Keshen gas reservoirs in the Kuqa Depression to study the phase mechanism. The EDFM and actual gas reservoir production performance are used to verify the effectiveness of the water invasion model [14–17]. Water invasion control measures for this kind of gas reservoir are put forward to improve the overall recovery rate of gas reservoirs. In 2018, Sun Xiongwei et al. established development technology countermeasures for single-well-controlled production pressure differences, with the early use of natural energy drainage and the later use of water production, according to an understanding of the development law of the Kelasu gas field [18].

In 2019, Wu Yongping et al. analyzed the general characteristics of water invasion in the Kela 2 gas field, determined the direction of the incoming water, predicted the water invasion mode of unseen wells, and put forward development countermeasures for waterproof water control [19]. In 2014, Dai Yong et al. conducted a water control test on the gas reservoir in the Dixi 18 well area with the most intensive water production and achieved good results [20]. In 2019, Zeng Li et al. focused on an analysis of the effect of water invasion control, optimized the control countermeasures, and scientifically guided the drainage and gas recovery measures [21]. In 2019, Jiang Tongwen et al. studied the gas–water relationship and the water invasion law of gas reservoirs. The development countermeasures of “high-level well drilling, moderate production increase and early drainage” were formulated [22]. Liu Huaxun et al. used experimental and numerical simulation methods to provide specific countermeasures for the rational and effective development of edge and bottom water gas reservoirs [23]. Xu Xuan et al. studied fractured, water-bearing, and low-permeability gas reservoirs and proposed multiwell coordinated drainage gas recovery and water control. The development methods were “layering, zoning, and classification” [24,25]. Lv Zhikai et al. analyzed the connectivity of reservoirs and pointed out optimization countermeasures for the well pattern and production system of gas wells [26]. Li Guoxin et al. analyzed in depth the factors affecting the recovery

of tight gas reservoirs and established a development countermeasure system to match the characteristics of the gas reservoirs in the area, improving the recovery of tight gas reservoirs [27–30]. Fan H C et al. pointed out that, in the case of water invasion in fractured gas reservoirs, natural gas primarily exists in the forms of bypass sealing gas, barrier sealing gas, and water-blocking sealing gas [31]. Hu Y et al. elucidated the main reasons for the significant decrease in gas recovery after water invasion in fractured gas reservoirs. During the process of fracture water invasion, edge and bottom water will rapidly advance along the fracture, and simultaneously, the reservoir matrix will adsorb water. After matrix water absorption, the gas-phase permeability resistance of the reservoir matrix increases, leading to a reduction in gas recovery [32]. Feng X et al. indicated that the development of fractures accelerates the manifestation of water invasion in gas reservoirs. The water invasion pattern corresponding to the development of microfractures is significantly different from the water breakthrough in the presence of large fractures or the development of a network of small fractures [33]. Zhou M et al. summarized various physical simulation methods for simulating water invasion in fractured gas reservoirs and compiled an overview of various water control methods [34]. Hu Y et al. found that when there is a highly permeable channel between layers and that the water-blocking phenomenon is more severe in low-permeability layers and in peripheral reservoirs far from gas wells [35]. Tan Xiaohua et al. believed that for fractured gas reservoirs, with a high degree of reservoir heterogeneity, water invasion easily leads to water-blocking gas. Conversely, for gas reservoirs with relatively uniform reservoir properties, water invasion has a greater replenishing effect on reservoir energy than the weakening effect of water-blocking gas on reservoir energy [36]. Gao Shusheng et al. pointed out that bottom water invasion is greatly influenced by reservoir permeability. When the permeability is around 0.1 mD or lower, bottom water has little effect on the recovery factor. Conversely, the higher the permeability, the faster the bottom water invasion, and the lower the recovery factor [37]. Liu Qunming et al. pointed out that the development pattern of fractures determines the water invasion rate, gas–water distribution, and recovery factor [38].

Although many scholars at home and abroad have conducted a lot of research on the development of fractured low-porosity gas reservoirs, there are still however many development problems that have not been solved for the ultradeep, fractured, and low-porosity gas reservoirs in the Tarim Basin, which are mainly reflected in the following facts: (1) There is a certain change in geological understanding, a certain deviation in the reserve base, a large difference between the actual pressure drop rate and the prediction, and a large difference between the gas reservoir development rate and the prediction. (2) The water breakthrough time of the gas reservoir is much earlier than that of the scheme, and the productivity of gas well decreases greatly after water breakthrough. The key scientific problems causing this development problem are as follows: (1) The seepage mechanism of the “pore–fracture–fault” triple medium in fractured low-porosity sandstone gas reservoirs is not clear. (2) At present, the understanding of water invasion mechanism of gas reservoir is not clear, and the potential of remaining gas remains to be further analyzed. (3) There are differences in water control measures for different gas reservoirs, which need to be further clarified.

On the basis of the development problems and scientific problems existing in the development practice of ultradeep, fractured, and low-porosity gas reservoirs, the author starts with the geological characteristics of the reservoir, combines the dynamic characteristics of gas reservoir development and production, analyzes the laboratory test conditions, and uses the embedded discrete fracture numerical simulation technology (EDFM) to establish a fractured low-porosity sandstone gas reservoir. The numerical simulation model of the “hole–fracture–fault” triple-media gas reservoir clarifies the water invasion mode of the ultradeep, low-porosity, and fractured gas reservoir under the triple-media condition, analyzes the distribution characteristics and laws of the remaining gas, and proposes water control countermeasures under the different water invasion modes of this type of gas reservoir to improve the overall recovery rate of the gas reservoir. It provides theoretical

and technical support for the economic and efficient development of ultradeep gas fields in the Kuqa Depression.

2. Basic Geological Characteristics of Gas Reservoir

The Kuqa Depression is located in the northern part of the Tarim Basin. It is a super-imposed foreland basin dominated by Mesozoic and Cenozoic sediments. It is connected to the southern Tianshan fault fold belt by thrust faults in the north, the Tabei uplift in the south, the Yangxia sag in the east, and the Wushi sag in the west. The depression is divided into “two belts and one depression” from north to south, namely the Kelastrust belt, Baicheng sag, and Qiulitage thrust belt (Figure 1). The Kelastrust belt is the first row of thrust structures in the southern foot of the southern Tianshan Mountains. The north–south direction can be further divided into the Kela zone and the Keshen zone with the Kelastrust fault as the boundary. The east–west direction of the Keshen area can be divided into five sections according to the structural characteristics: the Awat section, the Bozi section, the Dabei section, the Keshen section, and the Kela section. The north–south direction is cut by multiple secondary thrust faults secondary to the Kelastrust fault, and six rows of structures are developed (Figure 2).

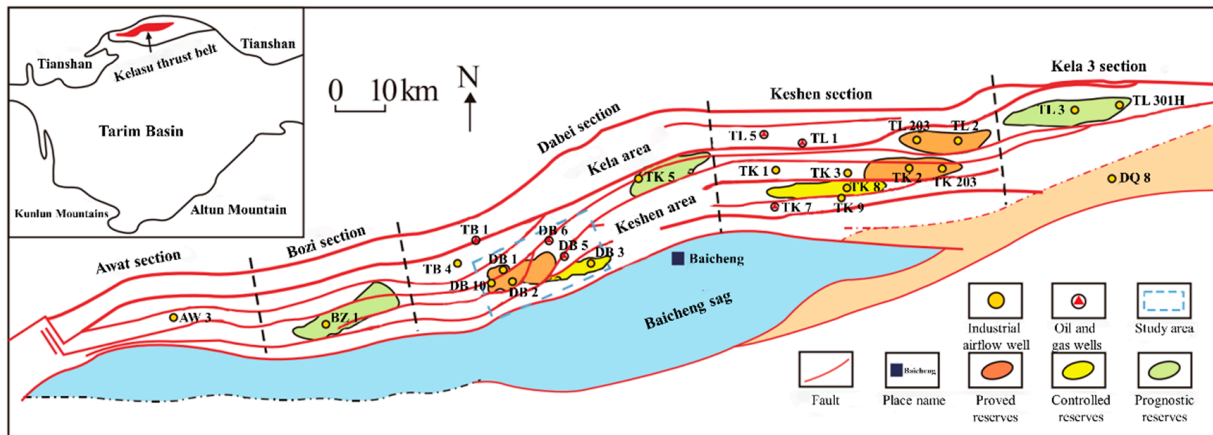


Figure 1. Division of structural units in Kuqa Depression (Revised according to reference [11]).

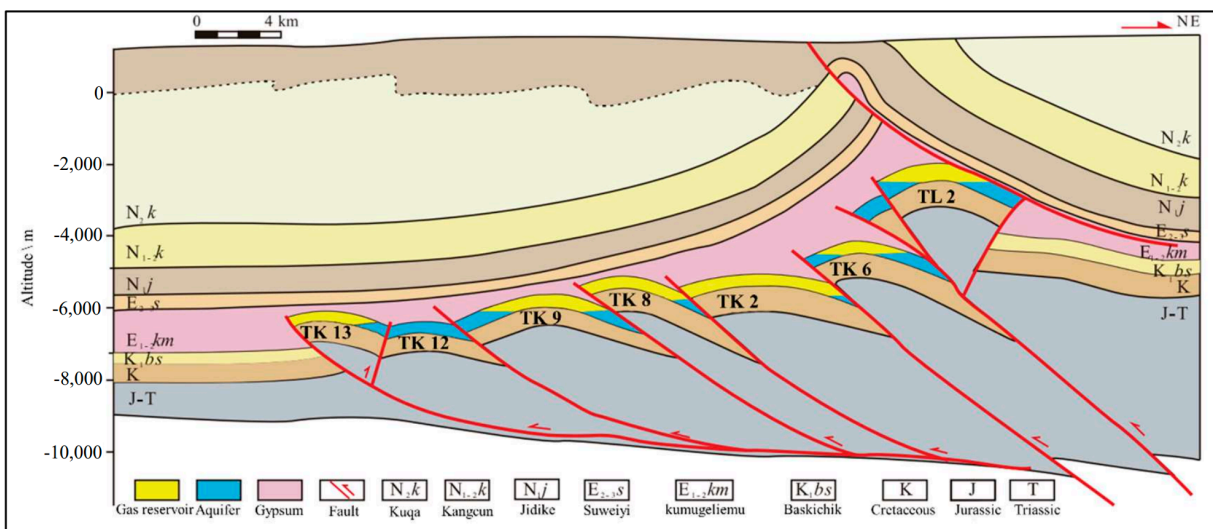


Figure 2. Gas reservoir profile of Kuqa Depression (revised according to reference [11]).

The main gas storage layer of the gas reservoir is the Cretaceous Bashijiqike Formation. The sedimentary facies are mainly braided river delta and fan delta deposits. The rock

types are mainly lithic feldspar sandstone, followed by feldspar lithic sandstone. The reservoir space is mainly dominated by intergranular pores (primary intergranular pores, intergranular dissolution enlarged pores), accounting for 62–72% of space. These are followed by intragranular dissolved pores, accounting for 14–18%. Micropores are well developed, accounting for 9–21%, and microfractures account for 1–2% (Figure 3). The average logging porosity of the reservoir is 5.4%. The average logging permeability is $0.055 \times 10^{-3} \mu\text{m}^2$, and the physical property difference is small. High-angle fractures are developed, and there is no obvious interlayer between reservoirs. Therefore, the Cretaceous Bashijiqike Formation is regarded as a set of vertically gas-bearing reservoirs. The average original formation pressure is 109.17 MPa, the average formation temperature is 152 °C, the static pressure gradient is 0.28 MPa/100 m, the temperature gradient is 2.16 °C/100 m, and the gas reservoir type is a layered edge water dry-gas reservoir with normal temperature and high pressure.

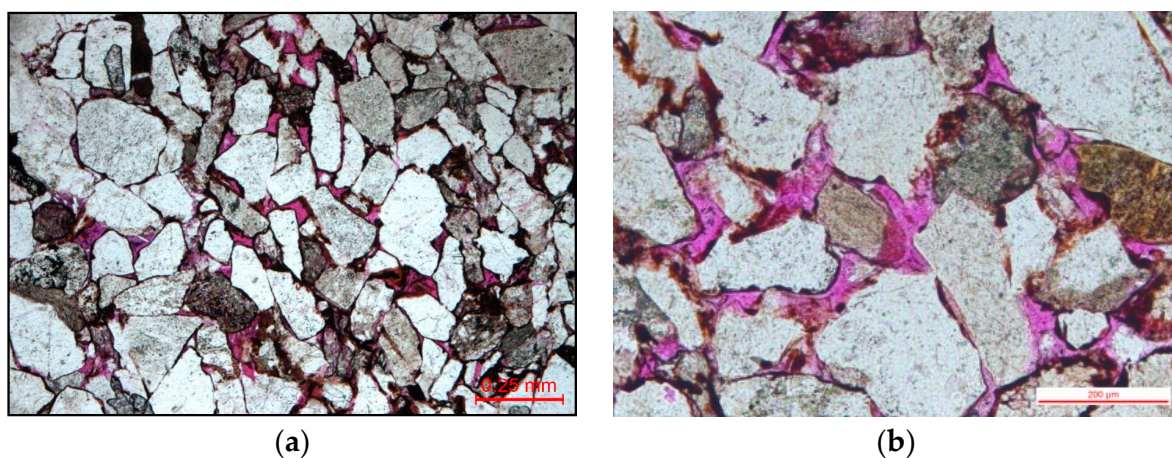


Figure 3. Cast thin sections of typical wells in Kuqa Depression gas reservoir. (a) KK505, 6776.81 m, primary intergranular pore. (b) KK501, 6428.85 m, intergranular dissolved pore.

3. Analysis of Water Invasion Characteristics of Gas Reservoir

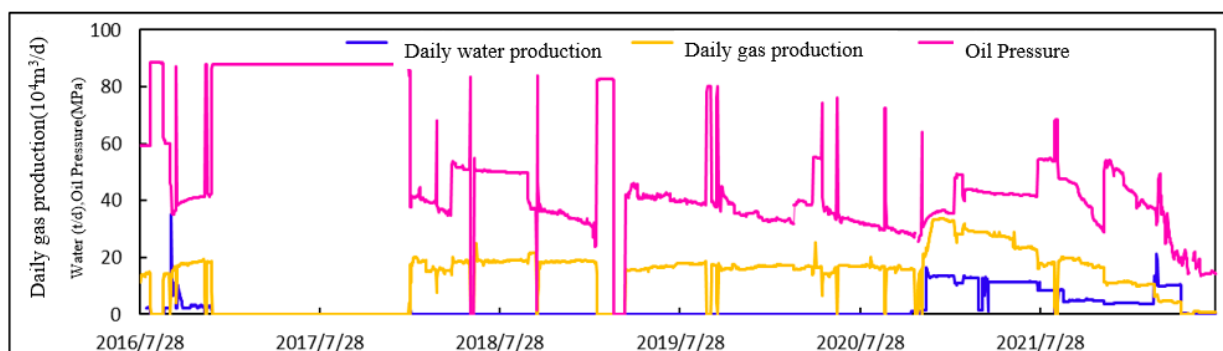
Since the development of gas reservoirs in the Kuqa Depression, some gas wells have suffered serious water invasion, and water invasion control is the top priority of the current work. Therefore, combined with the understanding of geological research, according to the production characteristics of the water-free gas production period, the average water–gas ratio, liquid-carrying production time, and water breakthrough or annual decline rate in the first year of production, the gas reservoir production wells can be divided into four categories, and the specific classification criteria are as shown in Table 1. The water invasion types of such gas wells are analyzed according to the water breakthrough characteristics and structural characteristics of different types of gas well. On the basis of the fracture development model of gas reservoirs, a foundation for the establishment of a water invasion model of gas reservoirs is laid in the next step.

The main characteristics and typical well water invasion characteristics of the four types of production wells in the Kuqa Depression gas reservoir are as follows.

The characteristics of Class I production wells are as follows: statistics Class I wells are mainly distributed in areas with a high degree of fracture development, far away from edge water, and close to structural highs. As shown in Figure 4, the TK5-2 well is located in the western structural high point of the K5 gas reservoir in the Kuqa Depression. The fracture network around the well is developed, far away from the edge and bottom water, and water has not been seen in production so far. However, with the advancement of production time, there is a risk of water invasion.

Table 1. Production well classification statistics of gas reservoir in Kuqa Depression.

Type	Productive Characteristic	Anhydrous Gas Recovery Period (Years)	Average Water–Gas Ratio	Liquid Carrying Time (Years)	The First Year of Water Annual Decline Rate (%)
Type-1	Waterless gas recovery period is long, water gas ratio is high, and water breakthrough time is late. At present, liquid-carrying production has been carried out, liquid-carrying production capacity is strong, and decline is slow.	>6	1.9~4.8	1.1~2.9	<10
Type-2	The water-free gas recovery period is long, the water–gas ratio is high, and the water breakthrough time is late. At present, liquid-carrying production has been carried out, with strong liquid-carrying production capacity and slow decline.	4~6	0.5~3.1	1.0~2.2	<15
Type-3	The water-free gas production period is short, the water–gas ratio is low, and the water breakthrough time is early, but at present, the liquid-carrying production has been carried out, the liquid-carrying production capacity is strong, and the decline is fast.	2~4	0.4~4.63	1.8~4.2	15~30
Type-4	The water-free gas production period is shorter, the water–gas ratio is higher, the water breakthrough time is earlier, the liquid-carrying production time is shorter, the water-flooded well is closed, and the decline is faster.	Basic < 3 years	Basic > 1.5 years	Basic < 1.5 years	>25

**Figure 4.** Production performance curve of TK5-2 well.

The characteristics of Class II production wells are as follows: statistics Class II wells are mainly distributed in areas with high fracture development and near structural highs. As shown in Figure 5, TK5-1 well is located in the western structural high of the K5 gas reservoir in the Kuqa Depression. In the early stage of production, the chlorine content was abnormal (more than 120,000 mg/L), and the water production was small but stable. After many measurements, there was no significant change in gas production and water production, which was comprehensively analyzed as reservoir retention water.

The characteristics of Class III production wells are as follows: statistics Class III wells are mainly distributed in areas with general fracture development, low structural parts,

and proximity to edge water. As shown in Figure 6, TK505 well is located in the middle and low part of the eastern structure of the K5 gas reservoir in the Kuqa Depression. The leakage and fracture network development degree of the whole well section are general. The production profile shows that the first member of Bayi is the main gas-producing water section. After water breakthrough, single wells basically have no water-carrying production capacity. The water invasion mainly involves water channeling along the fracture after the overall uplift of the edge and bottom water.

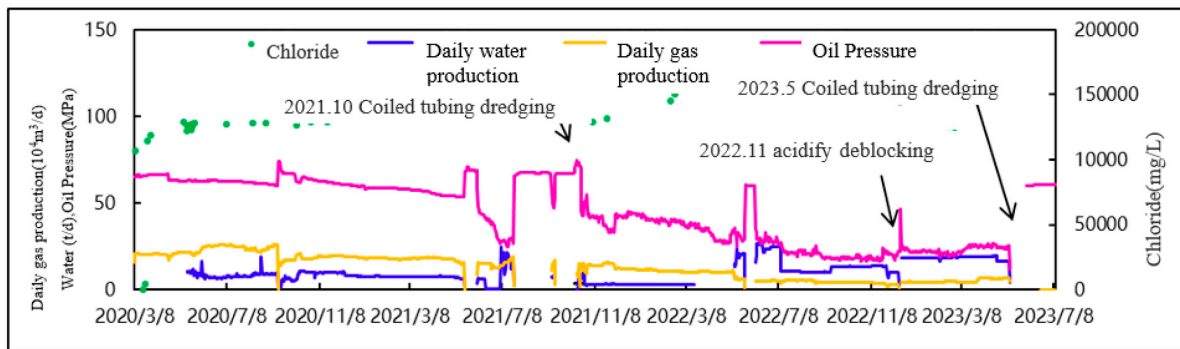


Figure 5. Production performance curve of TK5-1 well.

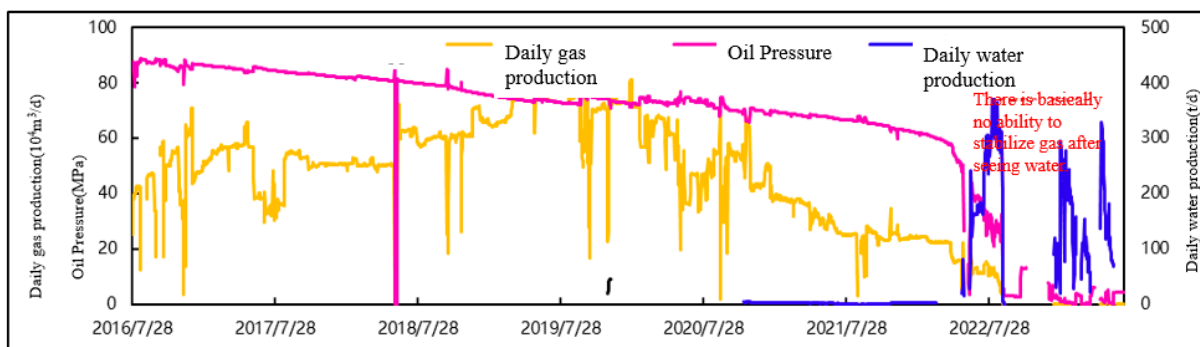


Figure 6. Production performance curve of TK505 well.

The characteristics of Class IV production wells are as follows: statistics of Class IV wells are distributed in the area near the edge water, near the fault, and through the cracks and faults. They are also prone to rapid water invasion and water flooding shut-in. As shown in Figure 7, TK5-3 well is located in the middle and lower part of the eastern structure of the K5 gas reservoir in the Kuqa Depression. The fracture effectiveness is poor and many large faults develop. The formation water invades nonuniformly along the large faults, resulting in rapid flooding of the TK5-3 well and causing it to shut down.

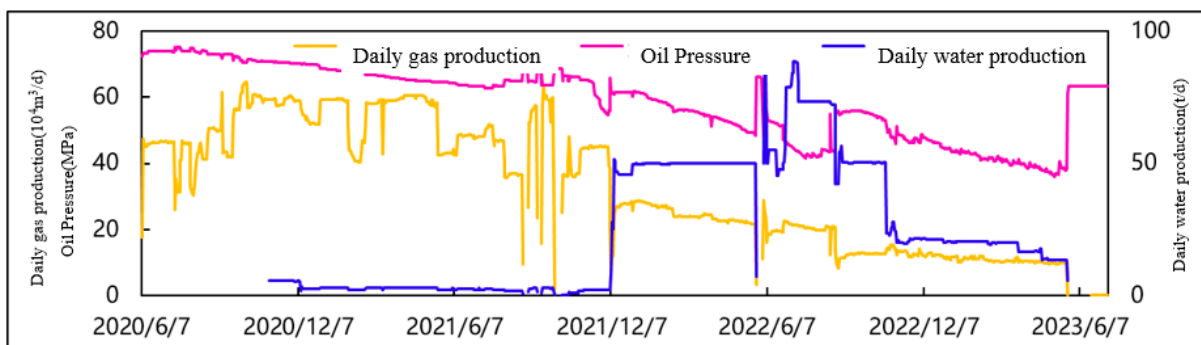


Figure 7. Production performance curve of TK5-3 well.

4. Large-Scale Physical Simulation Experiments on Water Invasion

Combining the characteristics of water invasion experimental devices, both domestically and internationally, a high-pressure, visualized, and large-scale physical water invasion experimental device has been developed. This device is used to conduct water invasion experiments under different fracture development modes and analyze various types of water invasion characteristics.

In this large-scale physical simulation experiment, fracture data from gas reservoirs are utilized, and corresponding fracture morphologies are cut out on artificial large plates using wire-cutting technology in order to create experimental models. The experimental simulation section is designed with a resistivity of 36 and pressure detection devices that can real-time detect and record the location and pressure changes of water intrusion into the rock plate. Additionally, it is equipped with a visualization window that facilitates the observation and recording of the water invasion process with a microscope.

The main simulation device is equipped with a mechanical device at the bottom that can adjust the angle, allowing for the simulation of development states under different formation dips. The injection end of the device is connected to an intermediate container, which simulates different sizes and pressures of edge and bottom water bodies. Furthermore, a porous media partition is installed at the bottom of the chamber, compensating for the limitations of conventional core point-wise water injection and enabling uniform contact between the water body and the bottom of the rock plate upon arrival, thus providing a more realistic simulation of edge and bottom water flooding.

4.1. Design of Large Physics Simulation Experimental Equipment

On the basis of the aforementioned design principles, a high-pressure visual water invasion physical simulation experiment device is developed. This device aims to overcome the limitations of nonvisualization in 2D core samples and the lack of 3D field mapping. It also provides visualization of the water invasion distance, ultimately yielding data that reflect oil and gas seepage parameters such as pressure and saturation fields. This allows for the analysis of water invasion patterns in three-dimensional space. The large-scale, high-pressure, visual water invasion physical experiment device comprises three major systems: a gas high-pressure injection system, a main visual simulation system, and a gas–water separation and measurement system. The structure of the device is illustrated in Figure 8.

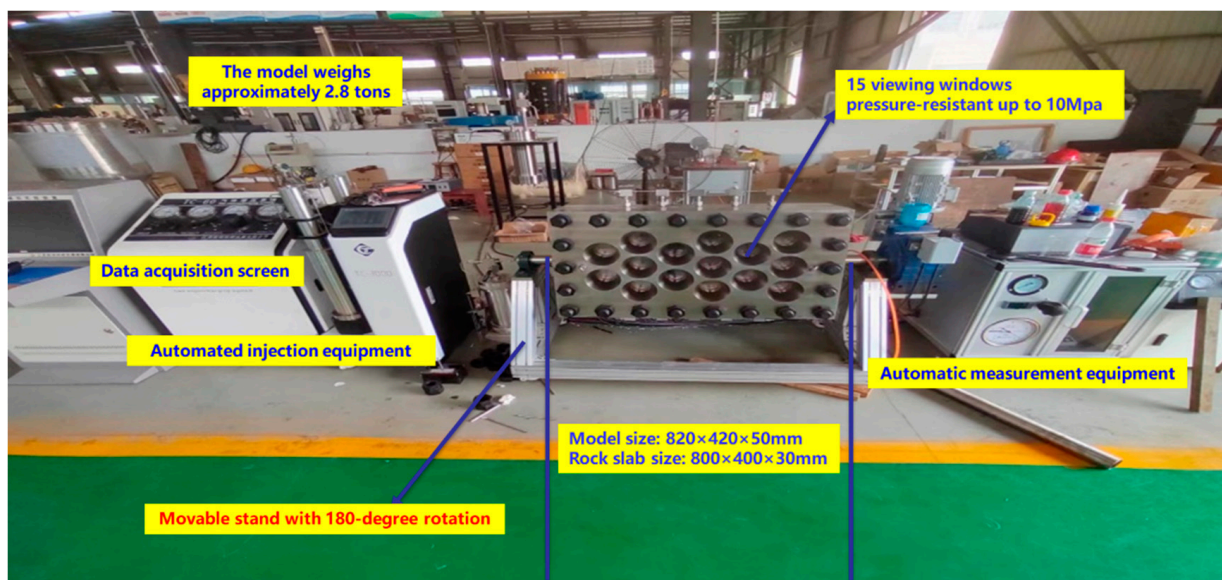


Figure 8. Physical simulation experimental equipment.

4.2. Physical Simulation Experiment Process

After the experimental simulations, a set of corresponding large-scale physical simulation experiment steps for water invasion are developed:

(1) Press Plate Fabrication and Fracture Creation

Manufacture artificial rock plates with different permeabilities (length 80 cm, width 40 cm, height 3 cm) using a mold. Use wire-cutting equipment to create fractures with different development patterns on the plates.

(2) Rock Plate Sand Sealing and Microscope Calibration

Seal the rock plate with tape on the sides and bottom, and then fill the fractures with sand. Perform final sealing with glue. Prepare river-grade glue for sealing around the rock plate. After sealing, press the simulation top onto the rock plate, and open the vent holes on the sides to vent the air inside the chamber, ensuring tight sealing between the rock plate and the cover. After the model is fully sealed, adjust the microscope's focal length to prepare for later observations of water invasion. Connect the pressure and saturation measurement points on the model and observe the measurement data to ensure accuracy.

(3) Saturation with Gas and Leak Testing

Increase the nitrogen pressure using an automatic high-pressure displacement pump. Open the high-pressure nitrogen source and charge the rock sample with nitrogen to 8 MPa. Let it sit for about 3 h, during which time nitrogen will be continuously injected through the displacement pump to step up the pressure to 8 MPa. Stabilize the experiment for more than 2 h, and then conduct leak testing to ensure no leakage. If no leakage is detected, the model has successfully returned to its original gas reservoir state.

(4) Edge Water Invasion in Rock Plates

Increase the pressure of the high-pressure water body to 8 MPa. Set a constant outlet pressure using the backpressure valve at the production end to simulate constant pressure drive in a production well. Achieve constant production by maintaining a stable production pressure difference. Stop production when the internal pressure of the flat model drops to 2 MPa.

(5) Data Collection

The data collection system can set collection time intervals and record production data: import and export pressure, water production, gas production, and cumulative water and gas production. It is necessary to connect measurement points on the back of the model, including 36 pressure and electrode measurement points. Then, measure pressure and electrode data at each point in the flat plate model in real time, and provide feedback to the data collection system. After the experiment, measure the invasion depth of the rock plate to calculate the invasion distance and sweep distance.

4.3. Analysis of Large Physical Simulation Experiment Results

Gas extraction speed is an important indicator to measure the speed of gas reservoir development. If the gas extraction speed is too small, it cannot fully tap into the potential of gas reservoir development. If it is too fast, it may shorten the steady production capacity, leading to faster water breakthrough and a rapid decline in production. Therefore, three different gas production rates were designed to analyze their impact on water invasion patterns in gas reservoirs.

Through conducting experiments on rock plates under different gas production rates, data on instantaneous gas production, stable production time, cumulative gas production, saturation levels, pressure, and other relevant parameters were obtained. On the basis of these data, an analysis was conducted on the impact of different gas production rates on water invasion patterns in gas reservoirs.

It can be seen from Table 2 that there are differences in the instantaneous gas production rules of gas wells under different gas production rates. The higher the gas production rate, the larger the instantaneous gas production at the early stage of production, and the closer the distance to the crack location, which is generally twice as large as that of well 1. At the same time, the steady production time is greatly shortened, indicating that the higher the gas production rate, the larger the driving pressure difference, and the faster the water invasion speed. This is further combined with saturation and pressure changes under different gas production rates to analyze the degree of gas utilization and the distribution of the remaining gas.

Table 2. Production data statistics under different gas production rates.

Gas Production Rate (%)	Instantaneous Gas Production (L/h)	Recovery Rate (%)	Time to Water Breakthrough (min)	Steady Production Time (min)	Water Production (g)
1	150	19.20	20.80	38.50	397
1.5	300	21.88	17.30	26.80	444.42
2	400	40.16	11	13.50	453.48
3	500	38.47	10.6	12.41	459.57
4	600	35.91	10.17	10.48	483.74
8	1000	30.40	9.14	9.76	549.47

It can be analyzed from pressure and saturation changes under different gas production rates that, as the gas production rate increases, the pressure at the crack location becomes higher. Under a 2% gas production rate, the average pressure at the crack is 3.6~3.8 MPa, and the pressure difference between the crack and matrix is 0.8~1.4 MPa. Under a 1.5% gas production rate, it is 3.45~3.6 MPa, and the pressure difference between the crack and matrix is 0.6~1.0 MPa. Under a 2% gas production rate, it is 3.2~3.55 MPa, and the pressure difference between the crack and matrix is 0.3~0.7 MPa, indicating that the crack is the channel for gas production. The larger the gas production rate, the larger the pressure difference between the matrix and crack, and the higher the utilization degree of gas in the matrix. The larger the gas production rate, the smaller the remaining amount of gas in the matrix. High-speed gas production results in residual gas being distributed in the middle, while low-speed gas production results in residual gas being distributed in matrices near water bodies.

It is further combined with production data such as cumulative gas production, water breakthrough time, steady production time, and recovery rate. According to experimental results of cumulative gas production of each scheme, a 2% gas production rate has a recovery rate of 40.16%, which is higher than that of 1% and 1.5% gas production rates. However, its water breakthrough time is 11 min, while that of a 1% gas production rate is 20.80 min. It can be seen that as the gas production rate increases, the cumulative gas production increases, water breakthrough time is advanced, water production is increased, and steady production time is shortened. Because of a small number of experimental design groups, under existing well-field development conditions, it is shown that as the gas production rate increases, cumulative gas production increases. Considering production data results, it is considered that a reasonable gas production rate is 2%.

It was found through experimental results that when the gas production rate is between 3 and 5%, with an increase in gas production rate, the recovery rate decreases, and steady production time shortens. Combined with changes in water breakthrough time and water production, it is concluded that a 2% gas production rate is the optimal gas production rate for the model. Continuously increasing the gas production rate leads to an increase in water invasion level and high initial gas production before opening a well, but fast water invasion speed causes the premature water inundation of wells. Additionally, because of a high gas production rate, it is difficult to extract gases that are blocked in the matrix by depressurization at later stages in the practical reservoir development process.

Therefore, in the actual reservoir development processes, reasonable gas production rates need to consider multiple indicators such as recovery rate, water breakthrough time, steady production time, water production, and other factors to reasonably plan reservoir gas production rates.

5. Research on Numerical Simulation of Embedded Discrete Fractures

To further investigate the water invasion characteristics of ultradeep, fractured, and low-porosity sandstone gas reservoirs in the Kuqa Depression, starting from actual gas reservoirs, this study analyzes the water invasion characteristics of gas reservoirs and characterizes water invasion patterns. On this basis, different embedded discrete fracture numerical simulation models for different water invasion types are established to analyze their water invasion mechanisms.

The water invasion form of fractured gas reservoirs mainly exhibits the characteristic of “water breakthrough”, where the production pressure difference causes the edge groundwater to quickly flow along high-permeability fractures to local gas wells. The larger the production pressure difference, the faster the water breakthrough occurs. The development of faults accelerates the occurrence speed and frequency of water breakthrough. Fractured water breakthrough can lead to many gas wells producing formation water in a short time, but these are soon flooded. After the ultradeep gas reservoirs in the Kuqa Depression are put into development, gas wells at low and high positions of the structure produce water to different degrees. Faults and fractures are the preferred channels for water invasion. The distance between production wells and edge groundwater, as well as the development degree of fractures and faults, jointly determine the intensity of gas well water production.

From the main characteristics of four types of production wells and typical water invasion characteristics of ultradeep gas reservoirs in the Kuqa Depression, it can be found that the gas reservoirs in the Kuqa Depression are typical heterogeneous water-injected gas reservoirs, which are jointly controlled by three factors: the structural location (the distance between the production well and the edge and bottom water), and the development degree of faults and fractures. Three types can be summarized: violent water flooding and channeling along faults (type I), uniform invasion along fractures or fracture networks (type II), and combined invasion along faults and fracture networks (type III).

With regard to the four types of production wells and typical water invasion characteristics of ultradeep gas reservoirs in the Kuqa Depression, it can be found that the gas reservoirs in the Kuqa Depression are typical heterogeneous water-injected gas reservoirs, which are jointly controlled by three factors: the structural location (the distance between the production well and the edge and bottom water), and the development degree of faults and fractures. Three types can be summarized: violent water flooding and channeling along faults (type I), uniform invasion along fractures or fracture networks (type II), and combined invasion along faults and fracture networks (type III).

Type I: along-fault water invasion with violent water breakthrough. In this type, regardless of whether the structure is high or low, once large faults are developed around the well, violent water breakthrough will occur. The strength of the fault itself determines the amount of water production in the production well. If there are small faults, the gas well will produce water, normally with stable liquid production and low chloride content, in the produced fluid. As the pressure difference between the gas reservoir and water body gradually decreases, the daily water production gradually increases, and, ultimately, the well is shut down because of an insufficient gas supply. If there are large faults, the well is prone to shutting down because of an insufficient gas supply after violent water breakthrough. The change rate of water content in the production reflects the size of the fault well, and the time of water breakthrough reflects the distance between the production well and the fault, which is closely related to the pressure difference between the gas reservoir and water body, and has a certain relationship with the structural location.

Type II: uniform invasion along fractures or fracture networks. As the Kuqa Depression belongs to low-porosity fractured gas reservoirs, fractures serve as the main migration channels. Therefore, its water invasion characteristics are clearly related to the structural location. Once water invasion occurs, it generally occurs within 1–2 years after water breakthrough. In this type of gas well, water invasion occurs as groundwater enters the wellbore along fractures. The chloride content in the produced fluid is high, and the time of water breakthrough or dry-gas production period is related to the structural location and pressure difference between the gas reservoir and water body. The lower the structural location, the faster the time of water breakthrough, and the smaller the pressure difference between the gas reservoir and water body, the faster the time of water breakthrough. Therefore, wells that experience violent water breakthrough later are generally classified as this type of water invasion mode.

Type III: combined invasion along faults and fracture networks. Because of the highly developed faults and fractures in the Kuqa Depression, this type of water invasion mode is the most common and is the main mode that produces “water-sealed gas” effects. It has strong relationships with structural location, fault and fracture combinations, pressure difference between gas reservoirs and water bodies, etc. The water invasion characteristics of production wells fall between the first two types.

In order to establish a more accurate mechanism model for ultradeep, fractured, and low-porosity sandstone gas reservoirs and analyze their water invasion mechanisms, as well as study improving recovery efficiency and corresponding technical countermeasures for gas reservoirs, a numerical simulation model for embedded discrete fractures in ultradeep, fractured, and low-porosity sandstone gas reservoirs is proposed. On the basis of the previous analysis, three typical well mechanism models are established. Fracture initial morphology and physical parameters are extracted from actual gas reservoir fracture characteristics parameters, including fracture and well productivity characteristics and water breakthrough time and sequence. Adjusting fracture permeability to fit water breakthrough time and adjusting fracture opening to fit final water content require a two-step process where corrections to fracture morphology and parameters mutually influence each other. Fine adjustments are needed to achieve expected modeling results. Fracture initial morphology is shown in Figure 9 and relevant data for mechanism models are shown in Table 3.

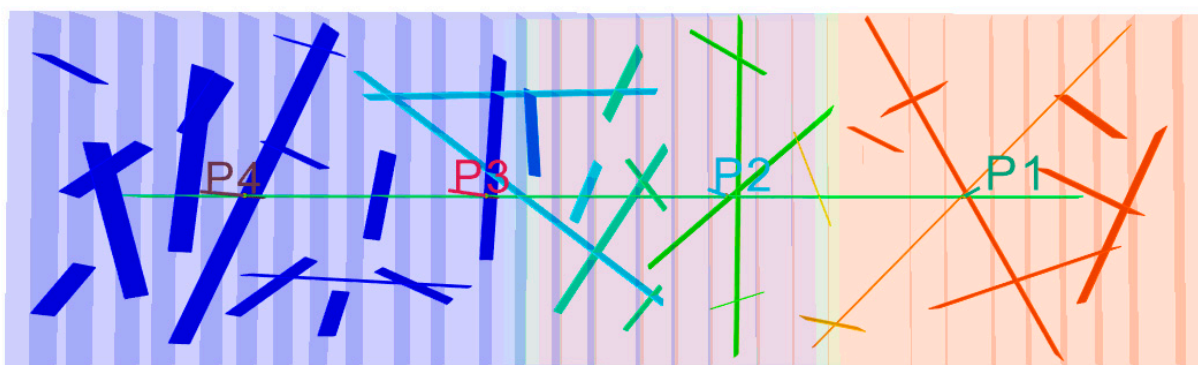


Figure 9. Initial morphology of fractures.

According to the current gas production rate of the actual gas reservoir and the gas production rate set in the large physical model, the numerical simulation sets the annual gas production rate at 1%, 1.5%, 2%, 3%, 4%, and 8% to comprehensively analyze the optimal gas production rate for different types of water invasion patterns. As the gas production rate increases, the cumulative gas production and water production gradually rise, while the daily gas production and water production reach an inflection point when the gas production rate is 2%. This rate can provide a longer stable production time and a relatively low daily water production rate. Therefore, the numerical simulation model shows that a

gas production rate of 2% is the appropriate rate for gas reservoir development, as shown in Figure 10.

Table 3. Basic Parameters of the Mechanistic Model.

Parameter	Value
Grid Scale	100 × 30 × 10 (30,000)
Grid Size	40 × 40 × 20 m
Number of Faults	1 secondary fault
Number of Discrete Fractures	37
Matrix Properties	Perm = 0.5 mD, Por = 0.15
Model Inclination Angle	20°
Model Reserves	24.6 billion cubic meters
Number of Wells	4 development wells

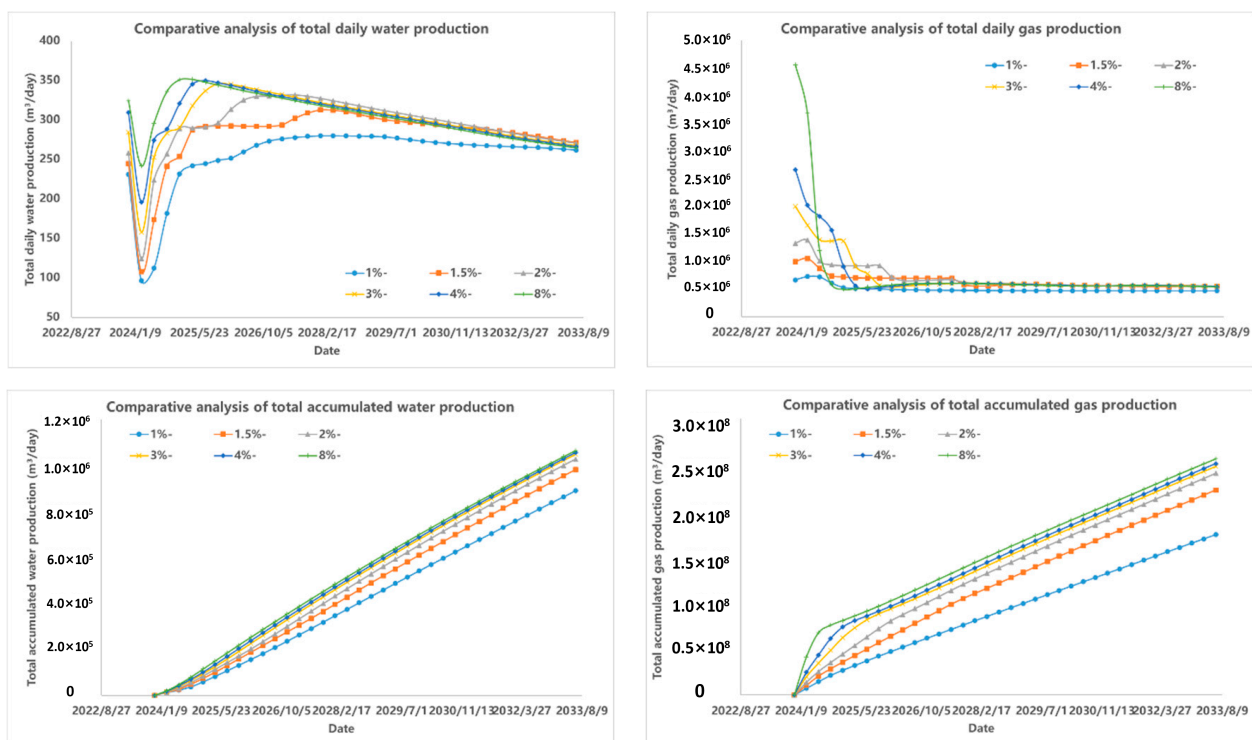


Figure 10. Analysis of numerical simulation results for different gas production rates.

6. The Development of Water Control Philosophy and Countermeasures in Gas Reservoirs

6.1. The Philosophy of Three-Dimensional Water Blocking and Combination of Water Blocking and Drainage

To further improve the overall recovery rate of the entire gas reservoir, a set of water control strategies based on three-dimensional water blocking and the combination of water blocking and drainage is established. On the basis of the mechanistic model, the application effects and mechanisms of this strategy are analyzed. After the first-line wells are plugged, the water body energy is significantly reduced, which improves the drainage effect. After the second-line wells are plugged, the water body energy continues to decrease. The specific development diagram is shown in Figure 11.

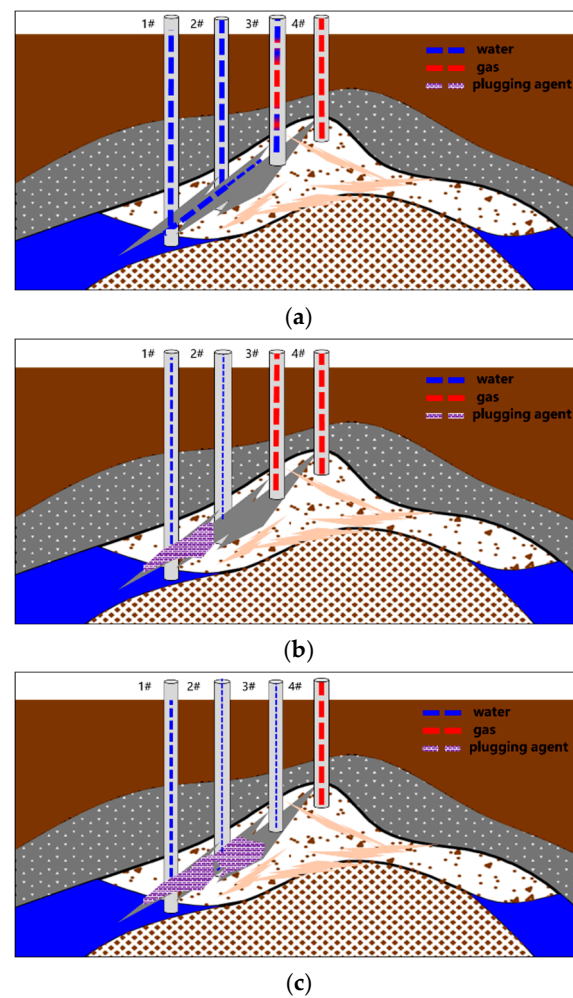


Figure 11. Schematic diagram of the three-dimensional water control strategy combining three-dimensional water plugging and drainage. (a) Stereogram of the energy restriction of strong water body on the effect of extraction. (b) Stereogram of initial first-line well plugging. (c) Stereogram of plugging of the second-line well in the later stage.

6.2. Three-Dimensional Water Blocking and Drainage Combined Water Control Measures

On the basis of the multiscale embedded discrete fracture numerical simulation model of TK gas reservoir in the Kuqa Depression, combined with the structural location, fault and fracture development characteristics of different production wells, four types of typical wells and three types of water invasion models are taken as the main objectives, and their historical production performance and predicted production performance characteristics are analyzed. According to the characteristics of different production wells, differentiated and ‘one well, one strategy’ implementation management are carried out.

On the basis of the geological characteristics, water invasion status, and residual gas enrichment of TK gas reservoir, four sets of schemes are designed for comparison and selection.

(1) Comparison Plan 1 (Old Well with Water Production).

A design to utilize natural gas reserves of $522.70 \times 10^8 \text{ m}^3$, annual gas production scale of $6.6 \times 10^8 \text{ m}^3$, with a total design of 15 wells, all of which are old wells (including 10 production wells and 5 monitoring wells). The predicted cumulative gas production at the end of the period is $108.79 \times 10^8 \text{ m}^3$, cumulative water production is $75.96 \times 10^4 \text{ t}$, and the predicted natural gas recovery rate at the end of the period is 20.81%.

(2) Comparison Plan 2 (5 old wells for drainage + 1 blocked well)

A design to utilize natural gas geological reserves of $522.70 \times 10^8 \text{ m}^3$, annual gas production scale of $6.6 \times 10^8 \text{ m}^3$. There are a total of 16 wells designed, including 15 old wells (including 10 production wells and 5 drainage wells) and 1 new well (including 1 reinjection well), with a daily drainage capacity of 900 t/d. The predicted cumulative gas production at the end of the period is $115.95 \times 10^8 \text{ m}^3$, cumulative water production is $272.40 \times 10^4 \text{ t}$, and there is a predicted natural gas recovery rate of 22.18% at the end of the period.

(3) Comparison Plan 3 (5 old wells for drainage, 4 new wells, and 1 blocked well)

A design to utilize natural gas geological reserves of $522.70 \times 10^8 \text{ m}^3$, annual gas production scale of $6.6 \times 10^8 \text{ m}^3$, with a total design of 19 wells, 15 old wells (including 10 production wells and 5 drainage wells), 4 new wells (including 3 production wells and 1 reinjection well), and a daily drainage capacity of 900 t/d. The predicted end-of-period cumulative gas production is $135.55 \times 10^8 \text{ m}^3$, the cumulative water production is $314.12 \times 10^4 \text{ t}$, and the predicted natural gas recovery rate at the end of the period is 25.93%.

(4) Comparison Plan 4 (4 old wells drainage + 4 new wells + 1 old well plugging)

A design to utilize natural gas geological reserves of $522.70 \times 10^8 \text{ m}^3$, annual gas production scale of $6.6 \times 10^8 \text{ m}^3$, with a total design of 19 wells, 15 old wells (including 10 production wells, 4 drainage wells, and 1 water blocking test well), 4 new wells (including 3 production wells and 1 reinjection well), a daily drainage capacity of 700 t/d, and a predicted cumulative gas production of $138.65 \times 10^8 \text{ m}^3$ at the end of the period, cumulative water production of $284.53 \times 10^4 \text{ t}$, and the predicted natural gas recovery rate at the end of the period is 26.52%.

On the basis of the research results of the comparative plan, taking into account factors such as the current increase in extraction degree, ground supporting facilities, and economic benefits, Plan 4 is recommended. Compared with Plan 1, Plan 4 accumulated a gas increase of 2.986 billion cubic meters and an increase in extraction degree of 5.1% (as shown in Figures 12 and 13).

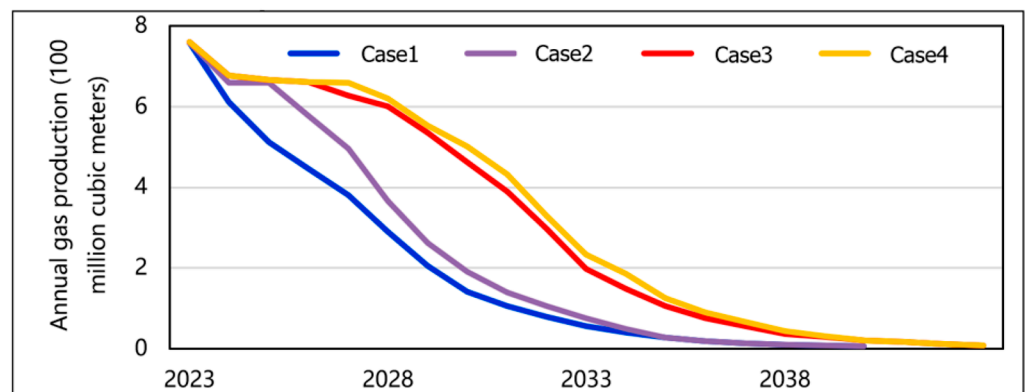


Figure 12. Annual Gas Production Comparison Curve of TK Gas Reservoir with Four Schemes.

In summary, for the production wells without water invasion, the main means of the efficient development of fractured water-bearing gas reservoirs is to adopt the water control countermeasures based on “prevention” and reasonably formulate the gas recovery rate. Through systematic research we found that, when the fracture development is relatively homogeneous, the reasonable gas recovery rate is between 2.0% and 2.4%. When the fracture development heterogeneity is strong, the reasonable gas recovery rate is smaller, between 1.6% and 2.0%. For water breakthrough wells, drainage is the main technical means of water control in gas reservoirs. However, for gas wells in different water invasion modes, there should be corresponding separate treatment. For the production wells with

violent water flooding along the fault, when the ‘harmonic plugging’ is the main method, the production interval of the gas well is adjusted, and the water channeling channel of the fault connecting the wellbore is blocked, and the effect is the best, which can effectively improve the recovery rate of the gas well. For the production wells with uniform invasion along fractures or fracture networks, the production rate of gas wells should be reasonably formulated, the production pressure difference should be controlled, and the drainage wells should be deployed or transformed at the bottom of the structure, so as to prolong the production period for the production wells in the middle and high parts.

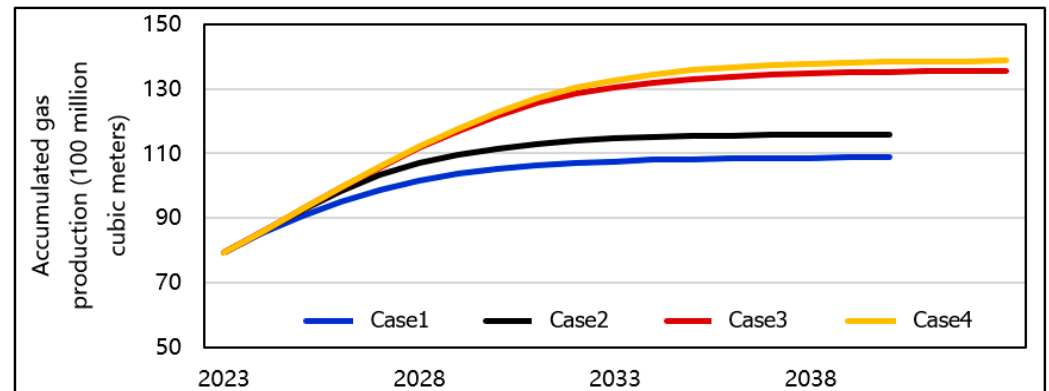


Figure 13. Comparison curves of cumulative gas production for four schemes of TK gas reservoir.

7. Conclusions and Outlook

7.1. Conclusions

(1) The production wells in the Kuqa Depression’s gas reservoirs can be categorized into four distinct groups based on key production metrics: water-free gas production duration, average water-to-gas ratio, duration of liquid-carrying production, and the rate of water breakthrough or annual decline during the initial production year. These classifications serve as the foundation for developing targeted water control strategies tailored to the unique characteristics of each gas reservoir.

(2) The gas reservoir in the Kuqa Depression exemplifies a nonuniform water invasion pattern, primarily influenced by three determining factors: structural positioning (specifically, the proximity of production wells to edge and bottom water sources), the prevalence and development of faults, and the presence of fractures. Illustrating this with the TK gas reservoir, we observe three distinct invasion patterns: violent water flooding along faults, uniform invasion through fracture networks, and a combined invasion pattern along both faults and fractures.

(3) Utilizing extensive physical simulation experiments and sophisticated discrete fracture numerical simulation models, we have observed a direct correlation between gas production rate and both stable production duration and water breakthrough time. Specifically, increased gas production rates lead to shorter stable production periods and accelerated water breakthrough. For the gas reservoirs under study, a gas production rate of 2% has been identified as the optimal balance, striking a crucial balance between production efficiency and reservoir sustainability.

(4) Taking into account the varied water invasion patterns observed in gas reservoirs, alongside the production dynamics and the strategic structural positioning of production wells, a comprehensive water control strategy has been devised. This strategy combines the principles of three-dimensional water blocking with a balanced approach of both water blocking and drainage. This results in a five-pronged water control approach encompassing “prevention, control, drainage, adjustment, and blocking.” Within this framework, a differentiated and tailored treatment approach is implemented for each well. Wells that have not yet experienced water invasion are primarily focused on preventive measures. Wells at risk of water invasion are managed with a focus on control. Wells that have already

been invaded by water undergo adjustment measures, whereas wells experiencing severe water breakthrough are targeted for blocking interventions. At the gas reservoir level, a “drainage and gas recovery” strategy is employed to effectively manage the water advance and thereby enhance the overall gas recovery rate. This integrated approach ensures that water control measures are tailored to the specific needs of each well and the gas reservoir as a whole, maximizing efficiency and effectiveness in gas production operations.

7.2. Outlook

After carefully examining the background and previous conclusions, it becomes evident that fractures and fracture networks play pivotal roles in both enhancing gas production and facilitating water invasion in gas reservoirs. Understanding the distribution of faults and fracture networks will be paramount in the development of such reservoirs, serving as a crucial stepping stone for future exploration efforts. Moreover, developing effective water control measures represents a significant challenge once the distribution of these features is clearly mapped out. Although drainage gas extraction has become the preferred method for developing smaller water-bearing gas reservoirs, larger reservoirs may benefit from a combined approach of blocking and removal techniques. This approach opens up a promising new avenue for the sustainable development of such reservoirs. However, the successful implementation of these strategies often hinges on the support of oilfield companies. Field testing and operational validation are essential for validating the effectiveness of these techniques, calling for a closer collaboration between researchers and industry professionals. This integration of engineering and technology represents a potential game changer for the future development of gas reservoirs, offering new hope for overcoming the challenges posed by water invasion.

Author Contributions: Conceptualization, D.C. and Y.W.; methodology, H.L.; software, C.Z.; validation, P.D., D.C. and Y.W.; formal analysis, D.C.; investigation, C.W.; resources, H.J.; data curation, C.Z.; writing—original draft preparation, M.Y.; writing—review and editing, H.L. and P.D.; visualization, P.D.; supervision, H.L.; project administration, M.Y.; funding acquisition, P.D. All authors have read and agreed to the published version of the manuscript.

Funding: This work was supported by Research Foundation of China University of Petroleum (Beijing) (Grant No. 2462019YJRC013).

Data Availability Statement: All the data have been presented in the article, there is no need to share the research data.

Conflicts of Interest: Author Dong Chen, Chengze Zhang, Min Yang, Haiming Li, Cuili Wang were employed by the company Tarim Oilfield Branch of PetroChina Company Limited. The remaining authors declare that the research was conducted in the absence of any commercial or financial relationships that could be construed as a potential conflict of interest.

References

1. Jia, C.; Pang, X. Research progress and main development direction of deep oil and gas geology theory. *Pet. J.* **2015**, *36*, 1457–1569.
2. Zhang, G.; Ma, F.; Liang, Y.; Zhao, Z.; Qin, Y.; Liu, X.; Zhang, K.; Ke, W. Global deep oil and gas exploration field and theoretical and technical progress. *Pet. J.* **2015**, *36*, 1156–1166.
3. Dkhimi, F.; Honda, A.; Hanson, K.; Mbau, R.; Onwujekwe, O.; Phuong, H.T.; Mathauer, I.; Akhnif, E.H.; Jaouadi, I.; Kiendrébéogo, J.A.; et al. Examining multiple funding flows to public healthcare providers in low- and middle-income settings: Results from case studies. *Int. J. Equity Health* **2023**, *22*, 123.
4. Maher, R.; Pedemonte-Rojas, N.; Gálvez, D.; Banerjee, S.B. The Role of Multistakeholder Initiatives in Radicalization of Resistance. *J. Manag. Stud.* **2023**, *58*, 1456.
5. Wang, Y.; Jiang, H.; Li, J. Study on water injection indicator curve model in fractured vuggy carbonate reservoir. *Geofluids* **2021**, *2021*, 1–14.
6. Bai, G.; Cao, B. Global deep oil and gas reservoirs and their distribution. *Pet. Nat. Gas Geol.* **2014**, *35*, 19–25.
7. Feng, J.; Gao, Z.; Cui, J.; Zhou, C. The exploration status and research progress of deep and ultra-deep clastic reservoirs. *Geosci. Prog.* **2016**, *31*, 718–736.
8. Sun, L.; Zou, C.; Zhu, R.; Zhang, Y.; Zhang, S.; Zhang, B.; Zhu, G.; Gao, Z. Formation, distribution and potential analysis of deep oil and gas in China. *Pet. Explor. Dev.* **2013**, *40*, 641–649. [[CrossRef](#)]

9. Zou, C.; Du, J.; Xu, C.; Wang, Z.; Zhang, B.; Wei, G.; Wang, T.; Wei, G.; Deng, S.; Liu, J.; et al. Formation, distribution, resource potential and exploration discovery of Sinian-Cambrian extra-large gas fields in Sichuan Basin. *Pet. Explor. Dev.* **2014**, *41*, 278–293. [[CrossRef](#)]
10. Lü, Z.; Tang, H.; Liu, Q.; Tang, Y.; Wang, Q.; Chang, B.; Nie, Y. Dynamic evaluation method of water-sealed gas in ultra-deep fractured tight gas reservoirs in Kuqa Depression, Tarim Basin. *Nat. Gas Geosci.* **2022**, *33*, 1874–1882. [[CrossRef](#)]
11. Jia, A.; Tang, H.; Han, Y.; Lv, Z.; Liu, Q.; Zhang, Y.; Sun, H.; Huang, W.; Wang, Z. Gas-water distribution and development strategy of deep gas field in Kuqa Depression, Tarim Basin. *Gas Geosci.* **2019**, *30*, 908–918.
12. Claudia, T.L.; Jesus, O.V. Potentially Toxic Cyanobacteria in a Eutrophic Reservoir in Northern Colombia. *Water* **2023**, *15*, 3696. [[CrossRef](#)]
13. Baryshev, I.A. First Find of the Invasive Amphipod *Gmelinoides Fasciatus* Basin Lake Vodlozero (Russ.). *Inland Water Biol.* **2023**, *16*, 860–862. [[CrossRef](#)]
14. Wang, Y.; Jiang, H.; Wang, Z.; Diwu, P.; Li, J. Study on the Countermeasures and Mechanism of Balanced Utilization in Multilayer Reservoirs at Ultra-High Water Cut Period. *Processes* **2023**, *11*, 3111. [[CrossRef](#)]
15. Sun, X.; Tang, Y.; Li, H.; Li, S.; Chen, L.; Zhang, W. 2018 National Natural Gas Academic Annual Conference. Oil and Gas Industry. 2018; 599–607. [[CrossRef](#)]
16. Wu, Y.; Yang, M.; Li, M.; Sun, Y.; Zhang, Y.; Wang, H. Water invasion law and model of Kela 2 gas field. *Xinjiang Pet. Geol.* **2019**, *40*, 302–306.
17. Dai, Y.; Qiu, E.; Shi, X.; Yan, Z.; Li, B.; Shi, Y.; Yang, D. Water invasion mechanism and countermeasures of the Kelameili volcanic gas field. *Xinjiang Pet. Geol.* **2014**, *35*, 694–698.
18. Zeng, L.; He, W.; Yang, S.; Chen, W.; Tong, L. Study on water invasion control countermeasures of Dongping bedrock gas reservoir. *China Pet. Chem. Ind. Stand. Qual.* **2019**, *2*, 176–177.
19. Jiang, T.; Sun, X. Development of Keshen ultra-deep and ultra-high pressure gas reservoirs in the Kuqa foreland basin, Tarim Basin: Understanding and technical countermeasures. *Nat. Gas Ind.* **2019**, *6*, 16–24. [[CrossRef](#)]
20. Xu, X.; Wan, Y.; Chen, Y.; Hu, Y.; Mei, Q.; Jiao, C. Experiment on water invasion mechanism and water control countermeasures of fractured edge water gas reservoir. *Nat. Gas Geosci.* **2019**, *30*, 1508–1518.
21. Duan, Y. Reasonable development technical countermeasures for fractured water-bearing gas reservoirs. *Oil Gas Field Surf. Eng.* **2009**, *28*, 22–23.
22. Lyu, Z.; Zhang, J.; Zhang, Y.; Yan, B.; Liu, Z.; Li, G. Connectivity of ultra-deep fractured tight sandstone gas reservoir and its development enlightenment-Taking Keshen 2 gas reservoir in Kuqa depression of Tarim Basin as an example. *Fault Block Oil & Gas Field.* **2023**, *30*, 31–37.
23. Li, G.; Tian, J.; Duan, X.; Yang, H.; Tang, Y.; Zhang, C.; Bi, H.; Xian, C.; Liu, H. The countermeasures and practice of greatly improving the recovery rate of ultra-deep tight sandstone gas reservoirs-Taking the Kelasu gas field in the Tarim Basin as an example. *Nat. Gas Ind.* **2022**, *42*, 93–100.
24. Li, B.; Zhu, Y.; Song, W.; Ji, G.; Xia, J. Establishment of productivity prediction equation for Kela 2 gas field. *Oil Explor. Dev.* **2004**, *31*, 107–111.
25. Sun, Z. Mining characteristics and development mode optimization of fractured water-bearing gas reservoirs. *Pet. Explor. Dev.* **2002**, *29*, 69–71.
26. Liu, H.; Ren, D.; Gao, S.; Hu, Z.; Ye, L.; Liu, X. Water invasion mechanism and development countermeasures of edge and bottom water gas reservoirs. *Nat. Gas Ind.* **2015**, *35*, 47–53.
27. Issaly, E.A.; Baranzelli, M.C.; Rocamundi, N.; FERREIRO, A.M.; Johnson, L.A.; Sérsic, A.N.; Paiaro, V. Unraveling the Worldwide Invasion of Tree Tobacco. *Biol. Invasions* **2023**, *25*, 2345.
28. Shi, Y.; Li, C.; Zhao, M.; Qin, G. Public Willingness to Pay for Farmland Non-Point Source Pollution Governance in China. *Sustain. Dev.* **2023**, *21*, 789.
29. Kukk, A.F.; Scheling, F.; Panzer, R.; Emmert, S.; Roth, B. Combined ultrasound and photoacoustic C-mode imaging system for skin lesion assessment. *Sci. Rep.* **2023**, *13*, 17947. [[CrossRef](#)] [[PubMed](#)]
30. Sun, K.; Szatmari, T.-I.; Pasta, A.; Bramsløw, L.; Wendt, D.; Christensen, J.H.; Pontoppidan, N.H. Daily sound exposure of hearing aids users during COVID-19 pandemic in Europe. *Front. Public Health* **2023**, *11*, 1091706. [[CrossRef](#)] [[PubMed](#)]
31. Fan, H.C.; Zhong, B.; Li, X.; Liu, Y.; Yang, H.; Feng, X.; Zhang, Y. Studies on water invasion mechanism of fractured-watered gas reservoir. *Nat. Gas Geosci.* **2012**, *23*, 1179–1184.
32. Hu, Y.; Li, X.; Wan, Y.; Jiao, C.; Xu, X.; Guo, C.; Jing, W. The experimental study of water invasion mechanism in fracture and the influence on the development of gas reservoir. *Nat. Gas Geosci.* **2016**, *27*, 910–917.
33. Feng, X.; Peng, X.; Li, L.; Yang, X.; Wang, J.; Li, Q.; Zhang, C.; Deng, H. Influence of reservoir heterogeneity on water invasion differentiation in carbonate gas reservoirs. *Tianranqi Gongye* **2018**, *38*, 67–75. [[CrossRef](#)]
34. Zhou, M.; Li, X.; Hu, Y.; Xu, X.; Jiang, L.; Li, Y. Physical simulation experimental technology and mechanism of water invasion in fractured-porous gas reservoir: A review. *Energies* **2021**, *14*, 3918. [[CrossRef](#)]
35. Hu, Y.; Li, X.; Shen, W.; Guo, C.; Jiao, C.; Xu, X.; Jia, Y. Study on the water invasion and its effect on the production from multilayer unconsolidated sandstone gas reservoirs. *Geofluids* **2021**, *2021*, 1–9. [[CrossRef](#)]

36. Tan, X.; Peng, G.; Li, X.; Chen, Y.; Xu, X.; Kui, M.; Li, Q.; Yang, G.; Xiao, H. Material balance method and classification of non-uniform water invasion mode for gas reservoirs with water considering the effect of water sealed gas. *Nat. Gas Ind.* **2021**, *41*, 97–103. [[CrossRef](#)]
37. Gao, S.; Yang, M.; Ye, L.; Liu, H.; Zhu, W. Simulation experiment of water invasion performance in low-permeability bottom water gas reservoir and its influence on recovery factor. *Nat. Gas Ind.* **2022**, *42*, 61–70.
38. Liu, Q.; Tang, H.; Lv, Z.; Wang, Q.; Liu, Z.; Chang, B. Study on gas-water distribution and water invasion law under different fracture development models in ultra-deep gas reservoir: Taking Keshen 2, 9 and 8 gas reservoirs of Tarim Basin as examples. *Nat. Gas Geosci.* **2023**, *34*, 963–972.

Disclaimer/Publisher's Note: The statements, opinions and data contained in all publications are solely those of the individual author(s) and contributor(s) and not of MDPI and/or the editor(s). MDPI and/or the editor(s) disclaim responsibility for any injury to people or property resulting from any ideas, methods, instructions or products referred to in the content.